Boundary Conditions for the Shallow Water Equations solved by Kinetic Schemes

Marie-Odile Bristeau, Benoit Coussin

INSTITUT NATIONAL DE RECHERCHE EN INFORMATIQUE ET EN AUTOMATIQUE

Boundary Conditions for the Shallow Water Equations solved by Kinetic Schemes

Marie-Odile Bristeau , Benoît Coussin

No 4282

Octobre 2001

THÈME 4

ISSN 0249-6399 ISRN INRIA/RR--4282--FR+ENG

INRIA
ROCQUENCOURT

Boundary Conditions for the Shallow Water Equations solved by Kinetic Schemes

Marie-Odile Bristeau *, Benoît Coussin †

Thème 4 — Simulation et optimisation
de systèmes complexes
Projet M3N

Rapport de recherche n ° 4282 — Octobre 2001 — 28 pages

Abstract: We consider the Saint-Venant system for Shallow Water which is an usual model to describe the flows in rivers, coastal areas or floodings. The hyperbolic system of conservation laws is solved on unstructured meshes using a finite volume method together with a kinetic solver. We add to this system a friction term, the role of which is important when small water depths are considered. In this paper we address the treatment of the boundary conditions, the difficulty is due to the fact that in some cases (fluvial flows) the given boundary conditions are not sufficient to apply directly the scheme, we discuss here how to treat these boundary conditions using a Riemann invariant. Some numerical results illustrate the ability of the method to treat complex problems like the filling up or the draining off of a river bed.

Key-words: Shallow water system, finite volume method, kinetic solver, friction, boundary conditions.

(Résumé : tsvp)

* M3N, Email : Marie-Odile.Bristeau@inria.fr
† M3N

Unité de recherche INRIA Rocquencourt
Domaine de Voluceau, Rocquencourt, BP 105, 78153 LE CHESNAY Cedex (France)
Téléphone : 01 39 63 55 11 - International : +33 1 39 63 55 11
Télécopie : (33) 01 39 63 53 30 - International : +33 1 39 63 53 30

Conditions aux limites pour le système de Saint-Venant résolu par un schéma cinétique

Résumé : On considère le système des équations de Saint-Venant qui modélise des écoulements en "eaux peu profondes" tels que dans les rivières, les zones côtières ou les crues. Ce système hyperbolique de lois de conservation est résolu sur des maillages non structurés par un schéma cinétique qui s'appuie sur une approche volumes finis. On prend aussi en compte un terme de friction dont le rôle est important quand on considère des zones à faible hauteur d'eau. Dans ce papier on traite en particulier le problème des conditions aux limites, la difficulté vient du fait que dans certains cas (écoulements fluviaux) les conditions imposées ne sont pas suffisantes pour appliquer directement le schéma, on montre ici comment traiter ces conditions en utilisant un invariant de Riemann. On montre les possibilités de la méthode sur des exemples comme la mise en eau et le découvrement du lit d'une rivière.

Mots-clé : Système de Saint-Venant, eaux peu profondes, volumes finis, schémas cinétiques, frottement, conditions aux limites.

1 Introduction

We study in this paper the problem of the boundary conditions for the Saint-Venant (or shallow water) system which is commonly used to model flows in rivers, lakes or coastal areas. In previous papers we have developed a solution method for this hyperbolic system of conservation laws, it is based on a finite volume approach and a kinetic solver. A useful property of this conservative scheme is the built-in preservation of the water depth positivity when applications with dry areas are considered. To find algorithms able to treat singular bottom topographies in all possible regimes is a very challenging problem for this system. In [1] we have emphasized the treatment of the source term due to the varying bed slope and proposed a scheme preserving steady states like the one of still water, the reader can see the references therein for several other approaches. A new kinetic approach is also proposed in [14] for the 1D problem. In [2] we have treated an additional equation for the simulation of the transport of a pollutant (or of temperature) and proposed a scheme preserving the conservation of pollutant and the monotonicity of its concentration.

We consider here the Saint-Venant system including a friction term, the role of which is important when small water depths are concerned, this term is treated by a semi-implicit scheme. In this paper we address particularly the treatment of the boundary conditions, the difficulty arising mainly for fluvial flows. Actually, in these cases, the given boundary conditions are not sufficient to apply directly the scheme on boundary edges. The idea proposed here is to use the one-dimensional problem projected in the direction normal to the boundary edge and to assume that the Riemann invariant related to the outgoing characteristic is constant along this characteristic. The problem of boundary conditions has been adressed by many authors, among others we can cite [4], [8], [11] who have considered the problem from different points of view.

In Section 2 we present the system of equations and its nonlinear hyperbolic structure, we introduce the kinetic formulation in Section 3 . The finite volume approach and a kinetic scheme are described in Section 4. In Section 5, we treat the friction term and in Section 6 we discuss on the boundary conditions. We recall some essential properties of the scheme in Section 7 and finally in Section 8 we show numerical results on examples with dry areas.

2 Equations

We consider the 2D Saint-Venant system, written in its physical conservative form (see Gerbeau and Perthame [7] for a derivation departing from the Navier-Stokes system),

$$\frac{\partial h}{\partial t} + \mathrm{div}(h\mathbf{u}) = 0, \tag{2.1}$$

$$\frac{\partial h\mathbf{u}}{\partial t} + \mathrm{div}(h\mathbf{u}\otimes\mathbf{u}) + \nabla(\frac{g}{2}h^2) + gh\nabla Z + g\frac{\mathbf{u}\,|\mathbf{u}|}{K^2 h^{\frac{1}{3}}} = 0, \tag{2.2}$$

where we denote $h(t,x,y) \geq 0$, the water depth, $\mathbf{u}(t,x,y) = \begin{pmatrix} u \\ v \end{pmatrix}$, the flow velocity, g the acceleration due to gravity intensity and $Z(x,y)$ the bottom height, and therefore $h+Z$ is the level of water surface (see Fig. 2.1). We denote also $\mathbf{q}(t,x,y) = \begin{pmatrix} q_x \\ q_y \end{pmatrix} = h(t,x,y)\mathbf{u}(t,x,y)$, the flux of water. For the friction term we use here the Strickler formula with K the Strickler coefficient.

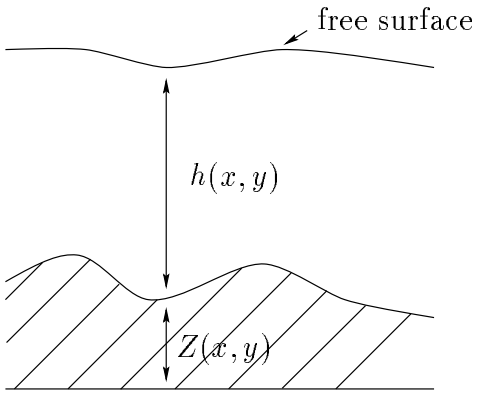

Figure 2.1:

To obtain a well-posed problem we add to this system some initial conditions

$$h(0,x,y) = h^0(x,y), \tag{2.3}$$
$$\mathbf{u}(0,x,y) = \mathbf{u}^0(x,y), \tag{2.4}$$

and boundary conditions. In this paper we consider only the following types of boundaries:

• Solid walls on which we prescribe a slip condition

$$\mathbf{u} \cdot \mathbf{n} = 0 \tag{2.5}$$

with $\mathbf{n}$ the unit outward normal to the boundary,

• Fluid boundaries on which we prescribe zero, one or two of the following conditions depending of the type of the flow (fluvial or torrential)

–Water level $h_g + Z$ given,

–Flux $\mathbf{q}_g$ given.

The system (2.1)-(2.2) of equations can be written as a system of first order conservation laws

$$\frac{\partial \mathbf{U}}{\partial t} + \text{div } \mathbf{F}(\mathbf{U}) = \mathbf{B}(\mathbf{U}), \tag{2.6}$$

with

$$\mathbf{U} = \begin{pmatrix} h \\ q_x \\ q_y \end{pmatrix}, \qquad \mathbf{F}(\mathbf{U}) = \begin{pmatrix} q_x & q_y \\ \frac{q_x^2}{h} + \frac{g}{2}h^2 & \frac{q_x q_y}{h} \\ \frac{q_x q_y}{h} & \frac{q_y^2}{h} + \frac{g}{2}h^2 \end{pmatrix}, \tag{2.7}$$

$$\mathbf{B}(\mathbf{U}) = \begin{pmatrix} 0 & \\ -gh\frac{\partial Z}{\partial x} & -g\frac{q_x\,|\mathbf{q}|}{K^2 h^{\frac{7}{3}}} \\ -gh\frac{\partial Z}{\partial y} & -g\frac{q_y\,|\mathbf{q}|}{K^2 h^{\frac{7}{3}}} \end{pmatrix}. \tag{2.8}$$

The system 2.6 can also be written in the non-conservative form

$$\frac{\partial \mathbf{U}}{\partial t} + \mathbf{A}_x \frac{\partial \mathbf{U}}{\partial x} + \mathbf{A}_y \frac{\partial \mathbf{U}}{\partial y} = \mathbf{B}(\mathbf{U}), \tag{2.9}$$

with $\mathbf{A}_x$ and $\mathbf{A}_y$ the Jacobian matrices

$$\mathbf{A}_x = \begin{pmatrix} 0 & 1 & 0 \\ -\frac{q_x^2}{h^2} + gh & \frac{2q_x}{h} & 0 \\ -\frac{q_x q_y}{h^2} & \frac{q_y}{h} & \frac{q_x}{h} \end{pmatrix}, \qquad \mathbf{A}_y = \begin{pmatrix} 0 & 0 & 1 \\ -\frac{q_x q_y}{h^2} & \frac{q_y}{h} & \frac{q_x}{h} \\ -\frac{q_y^2}{h^2} + gh & 0 & \frac{2q_y}{h} \end{pmatrix}. \tag{2.10}$$

For a given unit vector $\mathbf{n} = \begin{pmatrix} n_x \\ n_y \end{pmatrix}$, we will denote by $\mathbf{A}_n$ the Jacobian matrix "in direction $\mathbf{n}$" (see [9]) defined by

$$\mathbf{A}_n = \mathbf{A}_x n_x + \mathbf{A}_y n_y \tag{2.11}$$

i.e.

$$\mathbf{A}_n = \begin{pmatrix} 0 & n_x & n_y \\ (c^2 - u^2)n_x - uvn_y & 2un_x + vn_y & un_y \\ (c^2 - v^2)n_y - uvn_x & vn_x & 2vn_y + un_x \end{pmatrix} \tag{2.12}$$

where

$$c^2 = g\,h, \tag{2.13}$$

c represents the wave speed.

If we denote $u_n = un_x + vn_y$, the eigenvalues of $\mathbf{A}_n$ are $\lambda_1 = u_n - c$, $\lambda_2 = u_n$, $\lambda_3 = u_n + c$ and, for $h \neq 0$, the three eigenvalues are distinct and the system is strictly hyperbolic. A possible choice for the eigenvectors is

$$\mathbf{r}_1 = \begin{pmatrix} 1 \\ u - cn_x \\ v - cn_y \end{pmatrix}, \quad \mathbf{r}_2 = \begin{pmatrix} 0 \\ -n_y \\ n_x \end{pmatrix}, \quad \mathbf{r}_3 = \begin{pmatrix} 1 \\ u + cn_x \\ v + cn_y \end{pmatrix}. \tag{2.14}$$

We denote w_k the Riemann invariants, by definition they satisfy

$$\nabla_U w_k \cdot \mathbf{r}_k = 0, \quad k = 1, ..3. \tag{2.15}$$

The charateristic field associated to the eigenvalue λ_2 is linearly degenerated, actually we verify that:

$$\nabla_U u_n \cdot \mathbf{r}_2 = 0 \tag{2.16}$$

so we have $w_2 = u_n$.

A solution of (2.15) for $k = 1, 3$ is

$$w_1 = u_n - 2c \tag{2.17}$$

$$w_3 = u_n + 2c \tag{2.18}$$

We will use these properties for the treatment of the boundary conditions in Sec. 6.

3 Kinetic approach

In this section we do not take into account the friction term.

Following the studies of Perthame [12], Perthame and Qiu [13] on the kinetic schemes for gas dynamics, we introduce a kinetic approach to system (2.1)–(2.2) and in the next section we deduce from the discretization of the corresponding kinetic equation, a kinetic scheme for this system.

Let $\chi(w)$ be a positive, even function defined on $\mathbb{R}^2$ and satisfying

$$\int_{\mathbb{R}^2} \begin{pmatrix} 1 \\ w_i w_j \end{pmatrix} \chi(w)\, dw = \begin{pmatrix} 1 \\ \delta_{ij} \end{pmatrix} \tag{3.1}$$

with δ_{ij} the Kronecker symbol.

In addition we assume that $\chi(w)$ is compactly supported, i.e.

$$\exists w_M \in \mathbb{R}, \text{ such that } \quad \chi(w) = 0 \text{ for } |w| \geq w_M. \tag{3.2}$$

An example of function χ satisfying these properties is

$$\chi(w) = \frac{1}{12} \mathbb{1}_{|w_i| \leq \sqrt{3}}, \ i = 1, 2. \tag{3.3}$$

We introduce a microscopic density of particles $M(t, x, y, \xi)$ defined by a so-called *Gibbs equilibrium*

$$M(t, x, y, \xi) = \frac{h(t, x, y)}{\tilde{c}^2}\ \chi(\frac{\xi - \mathbf{u}(t, x, y)}{\tilde{c}}), \tag{3.4}$$

with $\tilde{c}$ defined by

$$\tilde{c}^2 = \frac{g\, h}{2}. \tag{3.5}$$

With these definitions we can write a kinetic interpretation of the system (2.1)–(2.2) and we have the following statement:

Theorem 3.1 *The functions $(h, \mathbf{q})$ are weak solutions to the system (2.1)–(2.2) or (2.6)–(2.7) if and only if $M(t,x,y,\xi)$ satisfies the kinetic equation*

$$\frac{\partial M}{\partial t} + \xi \cdot \nabla_x M - g \nabla Z \cdot \nabla_\xi M = Q(t,x,y,\xi), \tag{3.6}$$

for some "collision term" $Q(t,x,y,\xi)$ which satisfies for a.e. $(t,\ x, y)$,

$$\int_{\mathbb{R}^2} \begin{pmatrix} 1 \\ \xi \end{pmatrix} Q \ d\xi = 0. \tag{3.7}$$

Notice that the mathematical entropy property, for the energy, can also be considered in terms of the kinetic approach (see [14]).

Proof of Theorem 3.1. The proof relies on a very obvious computation. The two Saint-Venant equations are equivalent with the equation (3.6) once integrated in ξ against 1 and ξ. These are consequences of the usual relations deduced from the properties of χ and from (3.7):

$$\begin{pmatrix} h \\ \mathbf{q} \\ \dfrac{\mathbf{q}\otimes\mathbf{q}}{h} + \dfrac{g}{2}\, h^2 \mathbf{Id} \end{pmatrix} = \int_{\mathbb{R}^2} \begin{pmatrix} 1 \\ \xi \\ \xi \otimes \xi \end{pmatrix} M(\xi)\ d\xi, \tag{3.8}$$

and

$$\begin{pmatrix} 0 \\ h \end{pmatrix} = -\int_{\mathbb{R}^2} \begin{pmatrix} 1 \\ \xi \end{pmatrix} \nabla_\xi M(\xi)\ d\xi. \tag{3.9}$$

□

This theorem has a very fundamental consequence: the non-linear system (2.1)–(2.2) can be viewed as a linear transport equation on a nonlinear quantity M, for which it is easier to find a simple numerical scheme with good theoretical properties.

4 Kinetic scheme

A classical approach for solving hyperbolic systems consists in using finite volume schemes (see [9]) which are defined by the fluxes computed at the control volume interfaces. We show in this section how the fluxes of the kinetic scheme are deduced from the discretization of the kinetic equation (3.6).

4.1 Basic kinetic scheme

Let Ω denote the computational domain with boundary Γ, which we assume polygonal. In order to define the kinetic scheme, we introduce an usual finite volume discretization. Let $\mathcal{T}_h$ be a triangulation of Ω which vertices are denoted P_i. The dual cells C_i are obtained by

joining the centers of mass of the triangles surrounding each vertex P_i. We use the following notations (see Fig. 4.1):

K_i, set of nodes P_j surrounding P_i,
$|C_i|$, area of C_i,
Γ_{ij}, boundary edge belonging to cells C_i and C_j,
L_{ij}, length of Γ_{ij},
$\mathbf{n}_{ij}$, unit normal to Γ_{ij}, outward to C_i ($\mathbf{n}_{ji}$=-$\mathbf{n}_{ij}$).

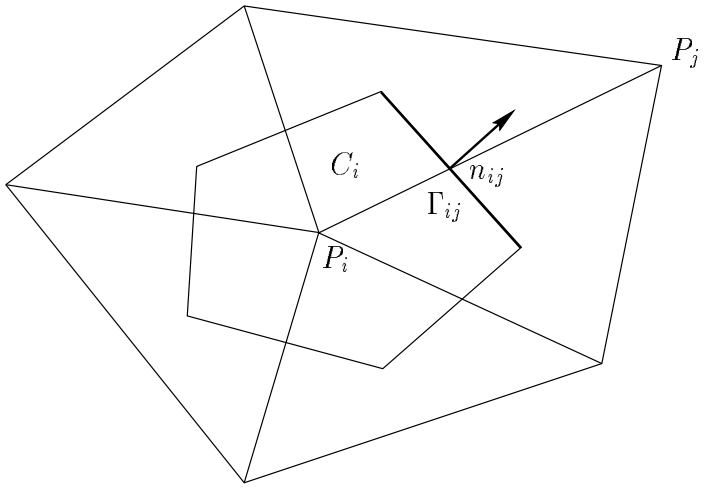

Figure 4.1: Dual cell C_i.

If P_i is a node belonging to the boundary Γ, we join the centers of mass of the triangles adjacent to the boundary to the middle of the edge belonging to Γ (see Fig. 4.2) and we denote

Γ_i, the two edges of C_i belonging to Γ,
$\mathbf{n}_i$, the unit outward normal defined by averaging the two adjacent normals.

Let Δt be the timestep, we set $t^n = n\ \Delta t$. We consider the system of equations (2.6) with $\mathbf{B} = 0$. We refer to [1] for a detailed description of the treatment of the terms due to the varying bed slope $gh\nabla Z$. We denote by $\mathbf{U}_i^n$ the approximation of the cell average of the exact solution at time t^n

$$\mathbf{U}_i^n \simeq \frac{1}{|C_i|}\int_{C_i} \mathbf{U}(t^n, x)\ dx. \tag{4.1}$$

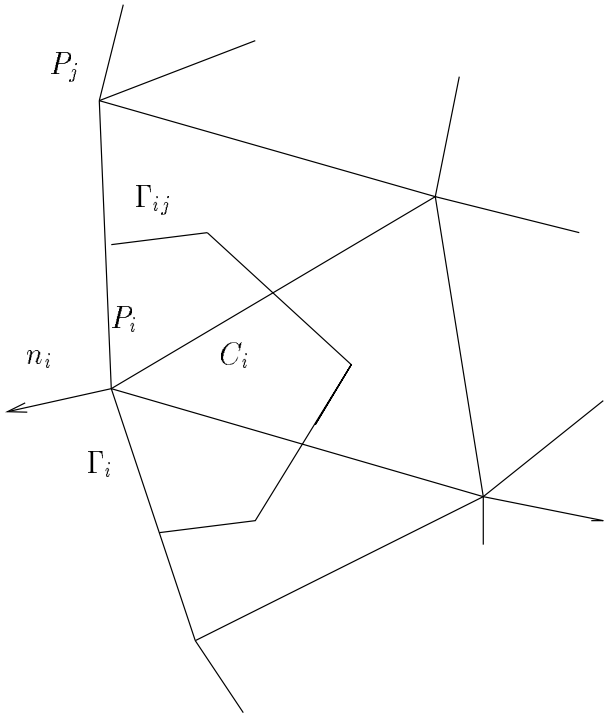

Figure 4.2: Boundary cell C_i.

We integrate in space and time the equation (2.6) on the set $C_i \times (t^n, t^{n+1})$, and, integrating by parts the divergence term, we obtain

$$\int_{C_i} \mathbf{U}(t^{n+1}, x)\ dx - \int_{C_i} \mathbf{U}(t^n, x)\ dx + \int_{t^n}^{t^{n+1}} \int_{\partial C_i} \mathbf{F}(\mathbf{U}) \cdot \mathbf{n}\ dxdt = 0. \tag{4.2}$$

So we can write

$$\mathbf{U}_i^{n+1} = \mathbf{U}_i^n - \sum_{j \in K_i} \sigma_{ij} \mathcal{F}(\mathbf{U}_i^n, \mathbf{U}_j^n, \mathbf{n}_{ij}) - \sigma_i \mathcal{F}(\mathbf{U}_i^n, \mathbf{U}_{e,i}^n, \mathbf{n}_i) \tag{4.3}$$

with

$$\sigma_{ij} = \frac{\Delta t\, L_{ij}}{|C_i|}, \qquad \sigma_i = \begin{cases} \dfrac{\Delta t\, L_i}{|C_i|} & \text{if } \mathrm{P_i} \in \Gamma, \\ 0 & \text{otherwise.} \end{cases} \tag{4.4}$$

and where $\mathcal{F}(\mathbf{U}_i, \mathbf{U}_j, \mathbf{n}_{ij})$ denotes an interpolation of the normal component of the flux $\mathbf{F}(\mathbf{U}) \cdot \mathbf{n}_{ij}$ along the edge Γ_{ij}. This interpolation is usually performed using a one dimen-

sional solver since locally the problem looks like a planar discontinuity. Here we define $\mathcal{F}(\mathbf{U}_i, \mathbf{U}_j, \mathbf{n}_{ij})$ using the kinetic interpretation of the system. The computation of the value $\mathbf{U}_{e,i}$ which denotes a value outside C_i defined such that the boundary conditions are satisfied and of the boundary flux $\mathcal{F}(\mathbf{U}_i, \mathbf{U}_{e,i}, \mathbf{n}_i)$ are detailed in Sec. 6. In the following of the present section we assume that P_i is an interior point. So, being given the solution $\mathbf{U}_i^n$ at time t^n for each cell, we compute $\mathbf{U}_i^{n+1}$ by the following algorithm with three steps:

- We define $M_i^n = M(h_i^n, hT_i^n, \xi - u_i^n)$ with M defined by (3.4).
- We use the microscopic equation (3.6). Since this equation is linear, we can apply a simple upwind scheme which defines a density function $f_i^{n+1}(\xi)$

$$f_i^{n+1}(\xi) - M_i^n(\xi) + \frac{\Delta t}{|C_i|} \sum_{j \in K_i} L_{ij}\ \xi \cdot \mathbf{n}_{ij}\ M_{ij}^n(\xi) = 0, \tag{4.5}$$

with the fluxes $M_{ij}^n(\xi)$ computed by the upwind formula

$$M_{ij}^n(\xi) = \begin{cases} M_i^n(\xi) & \text{for } \xi \cdot \mathbf{n}_{ij} \geq 0, \\ M_j^n(\xi) & \text{for } \xi \cdot \mathbf{n}_{ij} \leq 0. \end{cases}$$

Notice however that the density function $f(\xi)$ is not an equilibrium (see remark (4.1)).

- Nethertheless, we can recover the macroscopic quantities $\mathbf{U}_i^{n+1}$ at time t^{n+1} by integration

$$\mathbf{U}_i^{n+1} = \int_{\mathbb{R}^2} \begin{pmatrix} 1 \\ \xi \end{pmatrix}\ f_i^{n+1}(\xi)\ d\xi. \tag{4.6}$$

The numerical feasability of the method relies on the possibility to write directly a finite volume formula, which therefore avoids using the extra variable ξ in the actual implementation. Indeed, the equation (4.6) can be written with the form (4.3) with

$$\mathcal{F}(\mathbf{U}_i, \mathbf{U}_j, \mathbf{n}_{ij}) = \mathbf{F}^+(\mathbf{U}_i, \mathbf{n}_{ij}) + \mathbf{F}^-(\mathbf{U}_j, \mathbf{n}_{ij}), \tag{4.7}$$

and

$$\mathbf{F}^+(\mathbf{U}_i, \mathbf{n}_{ij}) = \int_{\xi \cdot \mathbf{n}_{ij} \geq 0} \xi \cdot \mathbf{n}_{ij}\ \begin{pmatrix} 1 \\ \xi \end{pmatrix}\ M_i(\xi)\, d\xi, \tag{4.8}$$

$$\mathbf{F}^-(\mathbf{U}_j, \mathbf{n}_{ij}) = \int_{\xi \cdot \mathbf{n}_{ij} \leq 0} \xi \cdot \mathbf{n}_{ij}\ \begin{pmatrix} 1 \\ \xi \end{pmatrix}\ M_j(\xi)\, d\xi. \tag{4.9}$$

Remark 4.1 *The interpretation is that, as usual, the collision terms Q, which forces the relaxation of f to Gibbs equilibrium M, is neglected in the advection scheme (4.5). And at each timestep we deduce $M_i^{n+1}(\xi)$ from $\mathbf{U}_i^{n+1}$ which is a way to perform all collisions at once and to recover the Gibbs equilibrium without computing them explicitely.*

4.2 Numerical implementation

We give here some details on the implementation of the kinetic scheme defined by (4.3), (4.7)-(4.9). For the efficiency of the method, we code in fact a variant where the choice of the function χ depends on the interface under consideration. For each edge Γ_{ij}, we define a local basis (n, τ) associated to the normal direction and to the tangential one. We denote $\hat{\mathbf{U}} = \begin{pmatrix} h \\ q_n \\ q_\tau \end{pmatrix}$, the vector deduced from $\mathbf{U}$ by the rotation in this new basis and $\hat{\mathbf{u}} = \begin{pmatrix} u_n \\ u_\tau \end{pmatrix} = \begin{pmatrix} \frac{q_n}{h} \\ \frac{q_\tau}{h} \end{pmatrix}$. If $\mathbf{n}_{ij} = (n_x, n_y)$, we have $\hat{\mathbf{U}}$ defined by

$$\hat{\mathbf{U}} = \mathbf{R}\ \mathbf{U} \quad \text{with} \quad \mathbf{R} = \begin{pmatrix} 1 & 0 & 0 \\ 0 & n_x & n_y \\ 0 & -n_y & n_x \end{pmatrix} \tag{4.10}$$

and

$$\mathbf{F}^+(\mathbf{U}, \mathbf{n}) = \mathbf{R}^{-1} \hat{\mathbf{F}}^+(\hat{\mathbf{U}}), \qquad \mathbf{R}^{-1} = \begin{pmatrix} 1 & 0 & 0 \\ 0 & n_x & -n_y \\ 0 & n_y & n_x \end{pmatrix}. \tag{4.11}$$

Using (4.8), we give the detailed expression of $\hat{\mathbf{F}}^+(\hat{\mathbf{U}}_i)$ related to the edge Γ_{ij}

$$\hat{\mathbf{F}}^+(\hat{\mathbf{U}}_i) = \frac{h_i}{\tilde{c}_i^2} \int_{(\xi_n \geq 0)\times \mathbb{R}} \xi_n \begin{pmatrix} 1 \\ \xi \end{pmatrix} \chi\left(\frac{\xi - \hat{\mathbf{u}}_i}{\tilde{c}_i}\right) d\xi \tag{4.12}$$

or, after the change of variables $w = \xi - \hat{\mathbf{u}}_i$,

$$\hat{\mathbf{F}}^+(\hat{\mathbf{U}}_i) = h_i \int_{(w_n \geq \frac{-u_{i,n}}{\tilde{c}_i})\times \mathbb{R}} (u_{i,n} + w_n\, \tilde{c}_i) \begin{pmatrix} 1 \\ u_{i,n} + w_n\, \tilde{c}_i \\ u_{i,\tau} + w_\tau\, \tilde{c}_i \end{pmatrix} \chi(w)\, dw. \tag{4.13}$$

Due to the fact that $\chi(w)$ is even, the term with w_τ disappears in (4.13) and we obtain the simpler formula

$$\hat{F}^+_{u_\tau}(\hat{\mathbf{U}}_i) = \hat{u}_{i,\tau}\ \hat{F}^+_h(\hat{\mathbf{U}}_i) \tag{4.14}$$

We obtain $\mathbf{F}^-$ by an analogous computation and so we have the same property for $\hat{\mathcal{F}}$. We will use this property to deduce a modified scheme with better accuracy.

4.3 Modified scheme

In order to reduce the diffusion of the scheme, we modify the computation of the flux related to the tangential component. For the computation of $u_{i,\tau}^{n+1}$ we replace the expression of $\hat{\mathcal{F}}$ by the following:

$$\hat{\mathcal{F}}_{u_\tau}(\hat{\mathbf{U}}_i, \hat{\mathbf{U}}_j) = u_{ij,\tau}\ \hat{\mathcal{F}}_h(\hat{\mathbf{U}}_i, \hat{\mathbf{U}}_j) \tag{4.15}$$

with

$$u_{ij,\tau} = \begin{cases} u_{i,\tau} & \text{for } \hat{\mathcal{F}}_h \geq 0, \\ u_{j,\tau} & \text{for } \hat{\mathcal{F}}_h \leq 0. \end{cases} \tag{4.16}$$

Formula (4.16) introduces some upwinding depending on the sign of the total flux. We give in [2] a numerical result showing the efficiency of (4.15).

The first order scheme defined in the previous section can be extended to a "formally" second order one using a MUSCL like extension (see [15]) with a Van Albada type limitor.

5 Friction

The friction term appears only in the momentum equation, we introduce a semi-implicit treatment of this term, then the equation (4.3) written for the variable $\mathbf{q}$ is replaced by

$$\mathbf{q}_i^{n+1} + g\Delta t \frac{|\mathbf{q}_i^n|\ \mathbf{q}_i^{n+1}}{K^2 h_i^n (h_i^{n+1})^{\frac{4}{3}}} = \mathbf{q}_i^n - \sum_{j \in K_i} \sigma_{ij} \mathcal{F}_q(\mathbf{U}_i^n, \mathbf{U}_j^n, \mathbf{n}_{ij}) - \sigma_i \mathcal{F}_q(\mathbf{U}_i^n, \mathbf{U}_{e,i}^n, \mathbf{n}_i). \tag{5.1}$$

If we denote $\tilde{\mathbf{q}}_i^{n+1}$ the right hand side of (5.1), we have

$$\mathbf{q}_i^{n+1} = \frac{\tilde{\mathbf{q}}_i^{n+1}}{1 + g\Delta t \dfrac{|\mathbf{q}_i^n|}{K^2 h_i^n (h_i^{n+1})^{\frac{4}{3}}}}\ . \tag{5.2}$$

6 Boundary conditions

In this section we describe the computation of the boundary flux $\mathcal{F}(\mathbf{U}_i^n, \mathbf{U}_{e,i}^n, \mathbf{n}_i)$ introduced in (4.3). The variable $\mathbf{U}_e$ represents the flow in a "fictitious" cell adjacent to the boundary. As in (4.7) we write

$$\mathcal{F}(\mathbf{U}_i^n, \mathbf{U}_{e,i}^n, \mathbf{n}_i) = \mathbf{F}^+(\mathbf{U}_i^n, \mathbf{n}_i) + \mathbf{F}^-(\mathbf{U}_{e,i}^n, \mathbf{n}_i) \tag{6.1}$$

with $\mathbf{U}_{e,i}^n$ defined following the type of the boundary.

In the following, we drop the superscript n and the subscript i to simplify the notations. For the computations we use the local coordinates as in section 4.2 and we will define $\hat{\mathbf{U}}_e = \begin{pmatrix} h_e \\ q_{e,n} \\ q_{e,\tau} \end{pmatrix}$.

6.1 Solid wall

If we consider a node P belonging to a solid wall, we prescribe a slip condition written

$$\mathbf{u} \cdot \mathbf{n} = 0. \tag{6.2}$$

We assume the continuity of the water depth and of the tangential component of velocity. We define

$$\hat{\mathbf{U}}_e = \begin{pmatrix} h \\ -q_n \\ q_\tau \end{pmatrix} \tag{6.3}$$

and from (4.13) we obtain

$$\hat{\mathbf{F}}^+(\hat{\mathbf{U}}) + \hat{\mathbf{F}}^-(\hat{\mathbf{U}}_e) = \begin{pmatrix} 0 \\ \frac{gh^2}{2} \\ 0 \end{pmatrix}. \tag{6.4}$$

The condition (6.2) is therefore prescribed weakly. It is possible to reinforce it by prescribing it a posteriori strongly. If we denote $\tilde{\mathbf{q}}^{n+1}$ the solution computed by (4.3) with (4.7)-(4.9) and (6.4), we then define

$$\mathbf{q}^{n+1} = \tilde{\mathbf{q}}^{n+1} - (\tilde{\mathbf{q}}^{n+1} \cdot \mathbf{n})\, \mathbf{n}. \tag{6.5}$$

We have to notice that, using (6.5), we can loose the conservation.

6.2 Fluid boundary

We recall that the type of a flow depends on the value of the Froud number $Fr = \dfrac{|\mathbf{u}|}{c}$, a flow is said

- torrential, for $|\mathbf{u}| > c$,
- fluvial, for $|\mathbf{u}| < c$.

Generally, for the fluid boundaries, the conditions prescribed by the user depend on the type of the flow defined by this criterium. For the treatment of the boundary conditions we will use actually the one dimensional projected system and consider the sign of the Jacobian matrix eigenvalues $u_n - c$ and $u_n + c$. Elsewhere, if we denote w_m the smallest number such that

$$\chi(w) = 0,\ \forall w \text{ such that } \quad |w_i| \geq w_m, i = 1, 2, \tag{6.6}$$

the kinetic scheme used here will be fully upwind or not, depending on the sign of $|u_n| - w_m \tilde{c}$. Despite this theoretical difficulty, we did not encounter numerical inconsistancies, in the following we will discuss how these different criteria interact and how the user's conditions can be satisfied according to the flow.

We have also to notice that with $\mathbf{n}$ the outward unit normal to the boundary edge, an inflow boundary corresponds to $\mathbf{u} \cdot \mathbf{n} < 0$ and an outflow one to $\mathbf{u} \cdot \mathbf{n} > 0$.

We will treat the following cases: for a fluvial flow boundary, we distinguish the cases where the flux or the water depth are given, while for a torrential flow we distinguish the inflow or outflow boundaries.

6.2.1 Fluvial boundary. Flux given

We consider first a fluvial boundary, so we assume that

$$|\mathbf{u}| < c. \tag{6.7}$$

If the flux $\mathbf{q_g}$ is given, then we wish to impose

$$\hat{F}_h^+(\hat{\mathbf{U}}) + \hat{F}_h^-(\hat{\mathbf{U}}_e) = q_{g,n}\,, \tag{6.8}$$

$$q_{e,\tau} = q_{g,\tau}. \tag{6.9}$$

To impose this directly leads to instabilities (especially because the numerical values are not necessarily in the regime of validity of this condition). We propose to discretize it in a weak form. We denote

$$a_1 = q_{g,n} - \hat{F}_h^+(\hat{\mathbf{U}}). \tag{6.10}$$

If $a_1 \geq 0$, we prescribe

$$\hat{F}_h^-(\hat{\mathbf{U}}_e) = 0 \tag{6.11}$$

and

$$\hat{F}_u^-(\hat{\mathbf{U}}_e) = 0. \tag{6.12}$$

If $a_1 < 0$, we have to write a third equation to be able to compute the three components of $\hat{\mathbf{U}}_e$. In this aim we use the one dimensional equations projected in the direction normal to the boundary edge. The system deduced from (2.6) with $\mathbf{B} = 0$ is then

$$\frac{\partial \hat{\mathbf{U}}}{\partial t} + \frac{\partial \hat{\mathbf{F}}(\hat{\mathbf{U}}) \cdot \mathbf{n}}{\partial x_1} = 0. \tag{6.13}$$

As (6.7) is satisfied, the eigenvalue $u_n + c$ of the projected system (see Sec. 2) is positive and we assume that the Riemann invariant related to the outgoing characteristic (positive eigenvalue in the local coordinates) is constant along this characteristic, i.e.

$$w_3(\hat{\mathbf{U}}_e) = w_3(\hat{\mathbf{U}}) \tag{6.14}$$

or

$$u_{e,n} + 2c_e = u_n + 2c. \tag{6.15}$$

We recall the notations $c = \sqrt{gh}$ and $\tilde{c} = \sqrt{\frac{gh}{2}}$.

We use the equations (6.8) and (6.15) to compute h_e and $u_{e,n}$. We denote

$$a_2 = u_n + 2c \tag{6.16}$$

and

$$m = \frac{u_{e,n}}{c_e}. \tag{6.17}$$

Then the equation (6.15) gives

$$\sqrt{g h_e}\ (m+2) = a_2 \tag{6.18}$$

and using the definition of $\hat{F}_h^-(\hat{\mathbf{U}}_e)$ (see(4.13)) and (6.8), (6.10) we have

$$h_e \int_{(w_n \leq \frac{-u_{e,n}}{\tilde{c}_e}) \times \mathbb{R}} (u_{e,n} + w_n\, \tilde{c}_e)\, \chi(w)\, dw = a_1 \tag{6.19}$$

or

$$\frac{(g h_e)^{\frac{3}{2}}}{\sqrt{2} g} \int_{(w_n \leq -\sqrt{2} m) \times \mathbb{R}} (\sqrt{2} m + w_n)\, \chi(w)\, dw = a_1. \tag{6.20}$$

If we denote

$$\phi(m) = \int_{(w_n \leq -\sqrt{2} m) \times \mathbb{R}} (\sqrt{2} m + w_n)\, \chi(w)\, dw, \tag{6.21}$$

we deduce from (6.20)

$$(g h_e)^{\frac{3}{2}} = \frac{\sqrt{2} g\ a_1}{\phi(m)} \tag{6.22}$$

and from (6.18), (6.22) we obtain the equation for m

$$\psi(m) = a_2 \tag{6.23}$$

where

$$\psi(m) = K \frac{(m+2)}{\phi(m)^{\frac{1}{3}}}. \tag{6.24}$$

with

$$K = (\sqrt{2} g\ a_1)^{\frac{1}{3}}. \tag{6.25}$$

We study in Annex A the functions $\phi(m)$ and $\psi(m)$ for the function $\chi(w)$ given by (3.3), we show that the equation has a unique solution for any a_2. We use a Newton algorithm to compute m solution of (6.23). Then from (6.17), (6.18) we deduce

$$h_e = \frac{1}{g} (\frac{a_2}{m+2})^2 \tag{6.26}$$

and

$$u_{e,n} = \frac{a_2 m}{m+2}. \tag{6.27}$$

Remark 6.1 *The condition (6.15) could be replaced by the conservation of the hydraulic head defined by (see [1])*

$$H = \frac{|u_n|^2}{2} + g(h + Z). \tag{6.28}$$

To obtain (6.28) we have considered also the 1D projected equation. The condition $H = Cst$ is valid only for steady states, so we have not developed here the computations with this condition (see [3]).

Remark 6.2 *We have assumed here that the flux q_g is prescribed locally, but in many computations only the global inflow or outflow flux is given. Then the user has to define a velocity profile and using the inflow or outflow surface we can deduce a local flux.*

6.2.2 Fluvial boundary. Water depth given

We verify that the flow is actually fluvial, i.e.

$$(u_n - c)(u_n + c) \leq 0. \tag{6.29}$$

We assume that the water depth is given, then we write

$$h_e = h_g. \tag{6.30}$$

We assume the continuity of the tangential component

$$q_{e,\tau} = q_\tau. \tag{6.31}$$

To define completely U_e, we assume, as in the previous case, that the Riemann invariant is constant along the outgoing characteristic (6.15), so we obtain

$$u_{e,n} = u_n + 2\sqrt{g}(\sqrt{h} - \sqrt{h_g}). \tag{6.32}$$

Sometimes it appears that the numerical values do not satisfy the condition (6.29), then the flow is in fact torrential and

- if $u_n > 0$, the condition (6.30) cannot be satisfied (see Sec. 6.2.4).
- if $u_n < 0$, one condition is missing, we will prescribe $u_{e,n} = u_n$.

6.2.3 Torrential inflow boundary

For a torrential inflow boundary we assume that the water depth and the flux are given, then we prescribe

$$h_e = h_g, \tag{6.33}$$

$$q_{e,\tau} = q_{g,\tau}, \tag{6.34}$$

and

$$\hat{F}_h^+(\hat{\mathbf{U}}) + \hat{F}_h^-(\hat{\mathbf{U}}_e) = q_{g,n}. \tag{6.35}$$

In this case we have to compute $q_{e,n}$ or $u_{e,n}$. We consider an inflow boundary, so $q_{g,n} < 0$ and by definition $\hat{F}_h^+(\hat{\mathbf{U}}) \geq 0$, therefore using the notation (6.10) we have

$$a_1 < 0. \tag{6.36}$$

By analogy with the previous section we denote

$$m = \frac{u_{e,n}}{c_g}, \tag{6.37}$$

then the equation for m is (see (6.19)-(6.22))

$$\phi(m) = \sqrt{\frac{2}{g}} \frac{a_1}{h_g^{\frac{3}{2}}}. \tag{6.38}$$

By definition of $\phi(m)$ (see Annex A) this equation has a unique solution $m < \frac{w_m}{\sqrt{2}}$ for $a_1 < 0$.

If $u_n \leq -w_m \tilde{c}$ implying that $\hat{F}_h^+(\hat{\mathbf{U}}) = 0$ and if $u_{g,n} \leq -w_m \tilde{c}_g$, we notice that $u_{e,n} = u_{g,n}$.

6.2.4 Torrential outflow boundary

In the case of a torrential outflow boundary, we prescribe no condition. We use the one dimensional projected equations (see Sec.2), and we assume that two Riemann invariants are constant along the outgoing characteristics (we assume that the two eigenvalues $u_n - c$, $u_n + c$ are positive, but in fact we have only $|\mathbf{u}| \geq c$). We obtain

$$u_{e,n} - 2\sqrt{gh_e} = u_n - 2\sqrt{gh}, \tag{6.39}$$

and

$$u_{e,n} + 2\sqrt{gh_e} = u_n + 2\sqrt{gh}, \tag{6.40}$$

and we deduce

$$h_e = h, \qquad u_{e,n} = u_n \tag{6.41}$$

We assume that we have also $q_{e,\tau} = q_\tau$. So in this case we obtain $\mathbf{U}_e = \mathbf{U}$.

For $u_n \geq w_m \tilde{c}$ we notice that $\mathbf{F}^-(\mathbf{U}_e) = 0$.

7 Properties of the scheme

It is clear from (4.3), (4.7)-(4.9) that the scheme is consistent and conservative and we have the following stability theorem:

Theorem 7.1 *Under the CFL condition*

$$\Delta t \leq \min \frac{|C_i|}{\left(\sum_{j \in K_i} L_{ij}\right) \left(|\mathbf{u}_i^n| + w_M \tilde{c}_i^n\right)}, \tag{7.1}$$

the kinetic scheme (4.3), (4.7)-(4.9) keeps the water depth positive. In (7.1) the minimun is taken on the values U_i^n of all the nodes and on the values U_e deduced from the boundary conditions.

Proof of Theorem 7.1. Suppose that we have $h_i^n \geq 0$. We consider the equation (4.5) used to define the kinetic scheme (4.3), (4.7)-(4.9). From the definition of the function M in (3.4) and the positivity of the function χ, we immediately deduce

$$M_i^n(\xi) \geq 0 \qquad \forall i.$$

We now introduce the quantities ξ_{ij}^+, ξ_{ij}^- defined by

$$\xi_{ij}^+ = \max(0, \xi \cdot \mathbf{n}_{ij}), \quad \xi_{ij}^- = \max(0, -\xi \cdot \mathbf{n}_{ij}),$$

and we rewrite the microscopic scheme (4.5) in the form

$$f_i^{n+1}(\xi) = (1 - \frac{\Delta t}{|C_i|} \sum_{j \in K_i} L_{ij}\ \xi_{ij}^+)\ M_i^n(\xi) + \frac{\Delta t}{|C_i|} \sum_{j \in K_i} L_{ij}\ \xi_{ij}^-\ M_j^n(\xi). \tag{7.2}$$

Then, for each node j, the value of ξ is either such that

$$|\xi - u_j^n| \geq w_M \tilde{c}_j^n$$

and then from the condition (3.2) on χ and the definition of function M we have

$$M_j^n(\xi) = 0,$$

or the value of ξ is such that

$$|\xi - u_j^n| \leq w_M \tilde{c}_j^n$$

which implies that $|\xi| \leq (|u_j^n| + w_M \tilde{c}_j^n)$ and then, using the relation $\xi_{ij}^+ \leq |\xi|$ and the CFL condition (7.1), we obtain

$$\frac{\Delta t}{|C_i|} \sum_{j \in K_i} L_{ij}\ \xi_{ij}^+ \leq 1.$$

Therefore, in the relation (7.2), $f_i^{n+1}(\xi)$ is a convex combination of nonnegative quantities and thus

$$f_i^{n+1}(\xi) \geq 0.$$

With a simple integration in ξ, we obtain

$$h_i^{n+1} \geq 0.$$

□

As we have shown in Section 6 that we apply the scheme also for the boundary nodes, we obtain by the way that the water depth positivity is preserved also for the boundary nodes. This stability property is important when applications with dry areas are considered as in the examples presented in Sec.8.

8 Numerical Results

The first example concerns a 2D rectangular channel with a parabolic bump on the bottom, this geometry has been used to compute steady states in a Workshop [6] initiated by Electricité de France, see also [1] for results on the same problems using the kinetic scheme

described in this paper. The channel length is L=25 m, the width is l=1 m and the bottom is modelized by the equation

$$Z(x,y) = \begin{cases} 0.2 - 0.05(x-10.)^2 & \text{if } 8 \text{ m} \leq x \leq 12 \text{ m}, \\ 0 & \text{elsewhere.} \end{cases} \tag{8.1}$$

The boundary of the computational domain is discretized with a space step equal to L/100 and the domain is discretized by an unstructured mesh with about 600 nodes and 1000 triangles.

We consider a 2D domain but the test case treated here simulates a 1D flow , this problem has been proposed in [5]. The initial condition is given by $h + Z = 0.5$ m and $\mathbf{q} = 0$. We consider the channel draining off, we assume that the left boundary is a solid wall like the two sides of the channel and we prescribe $h = 0.$ on the right boundary. We look at the unsteady solution leading to an equilibrium with $h + Z = 0.2$ m (top of the bump), $\mathbf{q} = 0.$ on the left of the bump and $h = 0.$, $\mathbf{q} = 0.$ on the right. We use the first order scheme and the time step is computed with CFL=1. We show in Figure 8.1 the side-view of the water level at different times, in Figure 8.2 we present the discharge at the same times. The flow is at first fluvial, then it is torrential on the bump, then this torrential part extend until the outflow boundary. For $t = 1000$ s we assume that the solution has converged to the steady state, the discharge is zero up to the machine accuracy.

We also have considered problems on a geometry given as test case in the code *Telemac* developed at EDF ([10]). It is a river with obstacles, the length is about 1,200 meters, the width 300 m, the bottom is varying from 252 to 260 m as shown in Figure 8.3(a). The mesh is about 1,000 nodes and 1,850 triangles. For the following computations we use as friction coefficient $K = 25$ m$^{\frac{1}{3}}$/s.

In a first example, we consider that the river bed is initially empty and by prescribing 254 m as water level on the inflow boundary we show the filling up of the river. We assume that the outflow boundary is replaced by a solid wall. For these two last examples we use the second order scheme, the time step is always computed with CFL=1. In Figures 8.3, 8.4 we present the water level at different times.

In the second example, we consider at the opposite the draining off of the river. The initial state is a constant water level (255 m) in the river as shown in Figure 8.5(a). We replace the inflow boundary by a solid wall and the prescribed outflow flowrate is growing from 0. to 500 m^3/s for t varying from 0 to 1800 s, then the flowrate is maintained equal to 500 m^3/s. Of course it is a global flowrate, so we prescribe also a constant velocity profile $\mathbf{u}_g = \alpha \begin{pmatrix} 1 \\ 0 \end{pmatrix}$. In fact the flowrate of 500 m^3/s is not reached due to the small waterdepth at the outflow boundary, the boundary condition becomes torrential and following Sec. 6.2.1 the code automatically switches to $\hat{F}^-(\hat{\mathbf{U}}_e) = 0$.

Animate solutions of these examples are shown in http://www-rocq.inria.fr/m3n.

9 Conclusions

In this paper we have proposed a method to treat the more usual boundary conditions for the Saint-Venant equations. It discretizes the given conditions in a weak sense and uses the same solver as the interior nodes. The same idea could be used for other finite volume schemes. An important property of the kinetic scheme used here is the preservation of the water depth positivity and this property is also satisfied at the boundary nodes.

Acknowledgements.

The authors would like to thank B. Perthame for deciding suggestions and comments. We also gratefully acknowledge the partial support of EDF/LNHE.

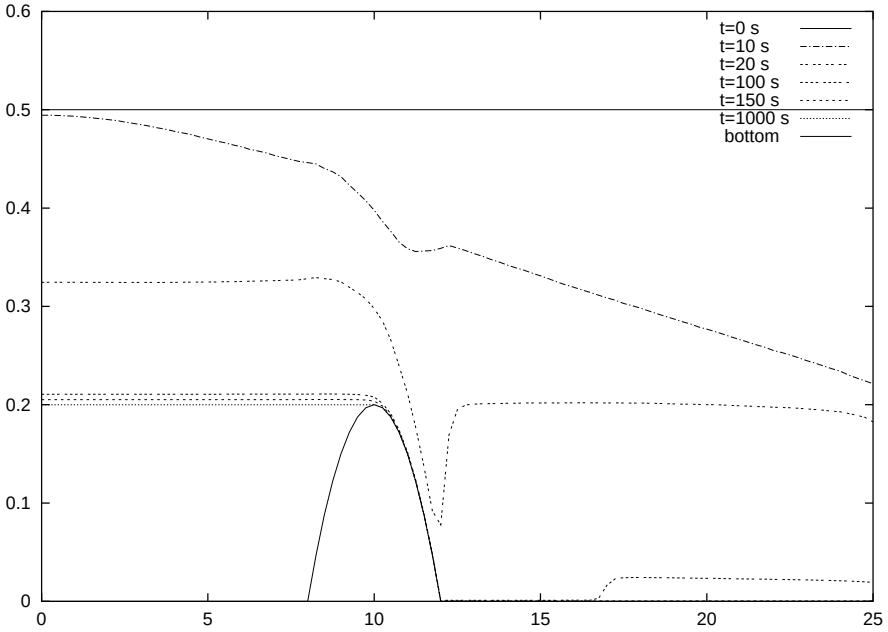

Figure 8.1: Draining off a channel with a bump. Water level at different times.

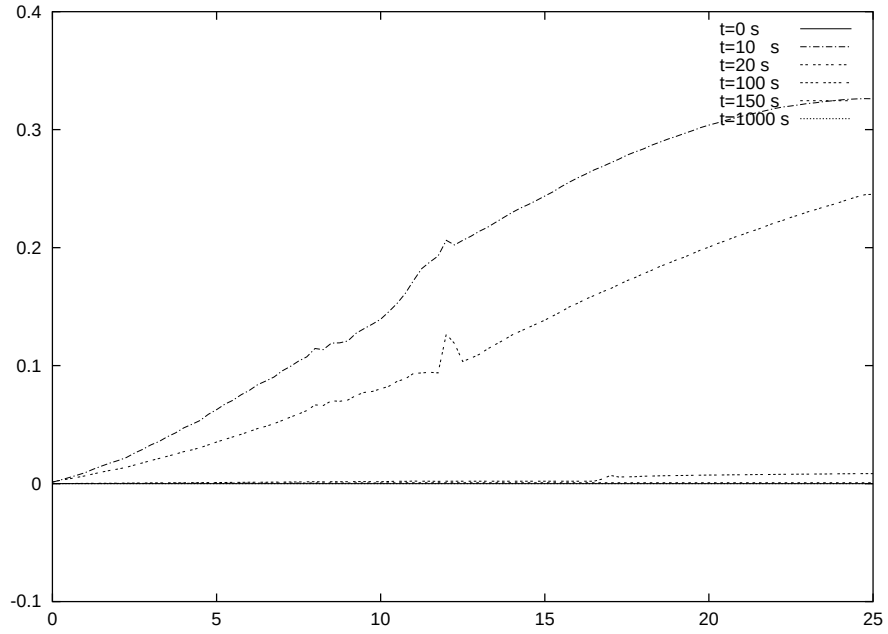

Figure 8.2: Discharge at different times.

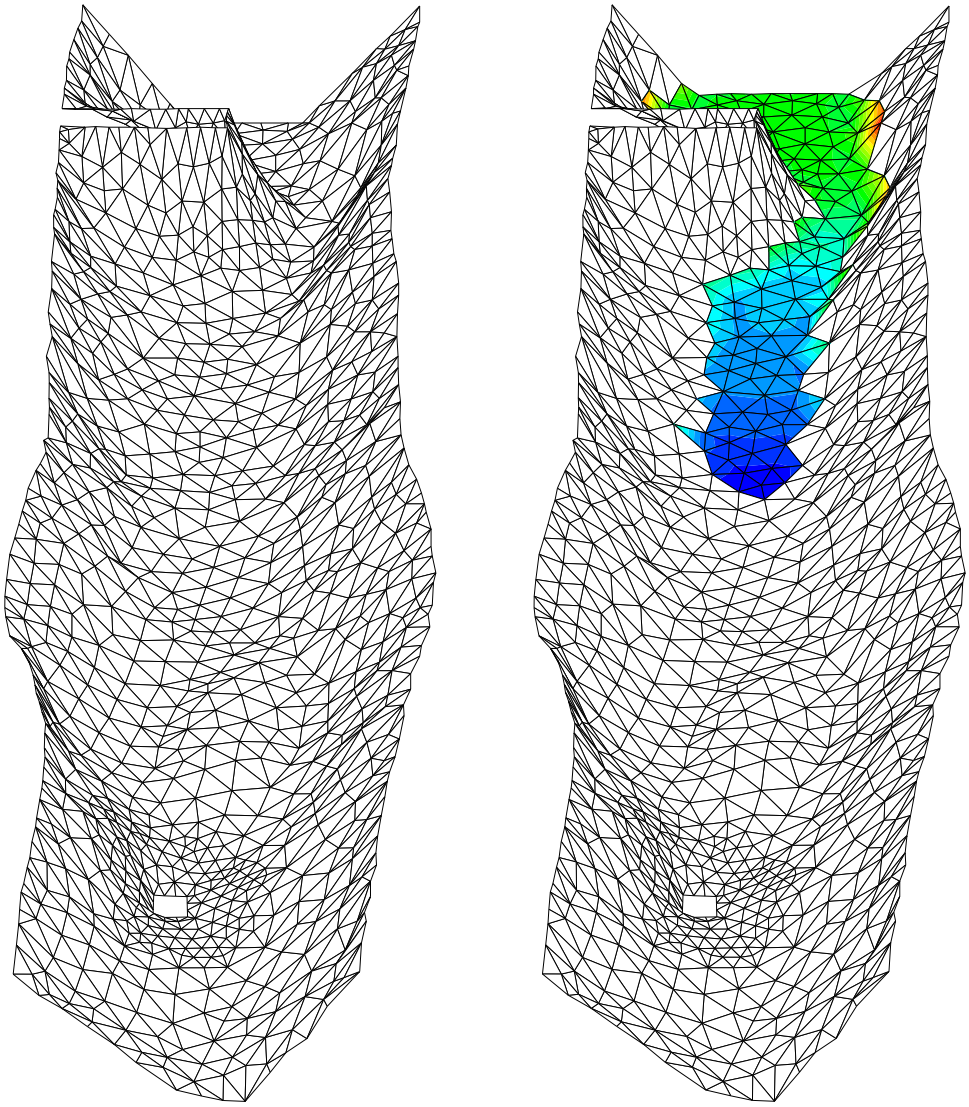

(a) Empty river bed

(b) $t = 200$ s

Figure 8.3: Filling up the river (1).

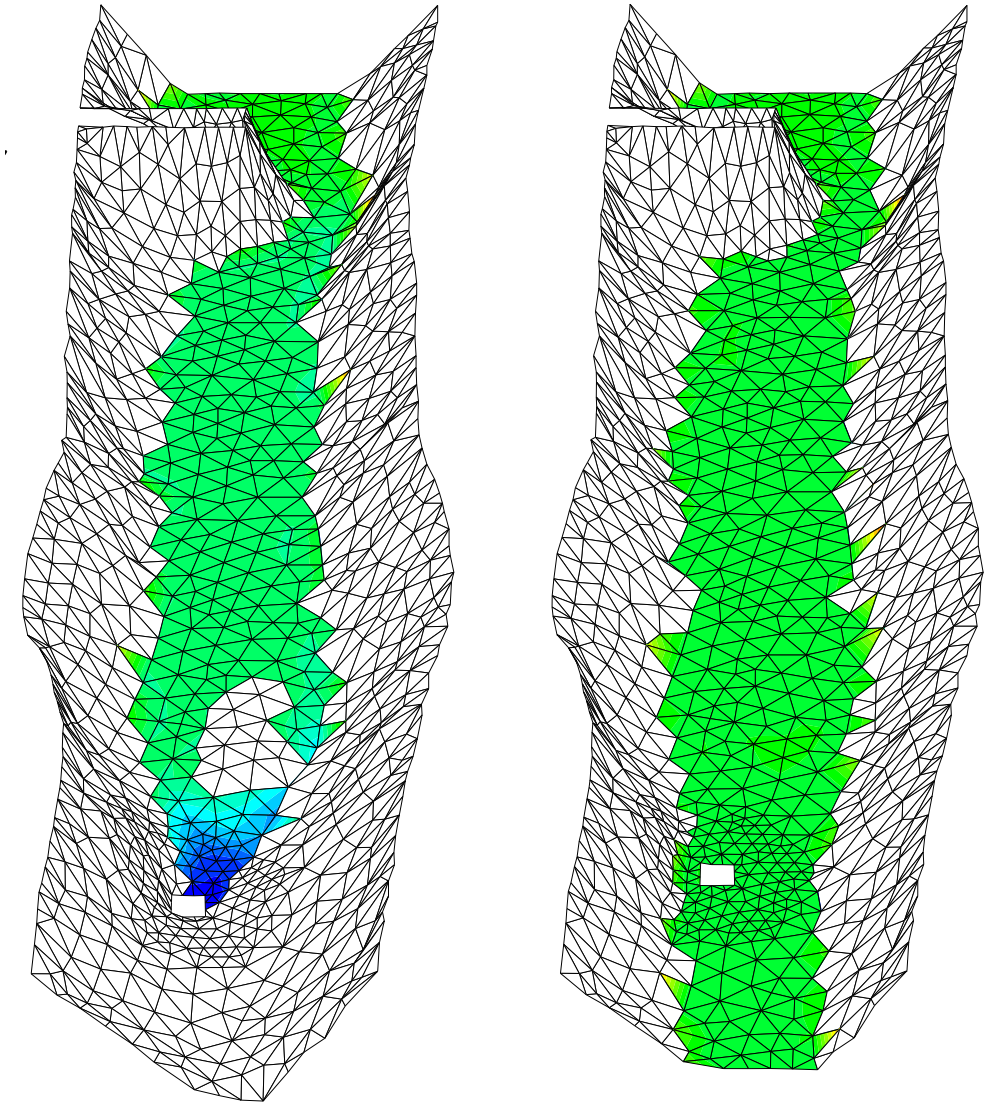

(a) $t = 2000$ s (b) $t = 5000$ s

Figure 8.4: Filling up the river (2).

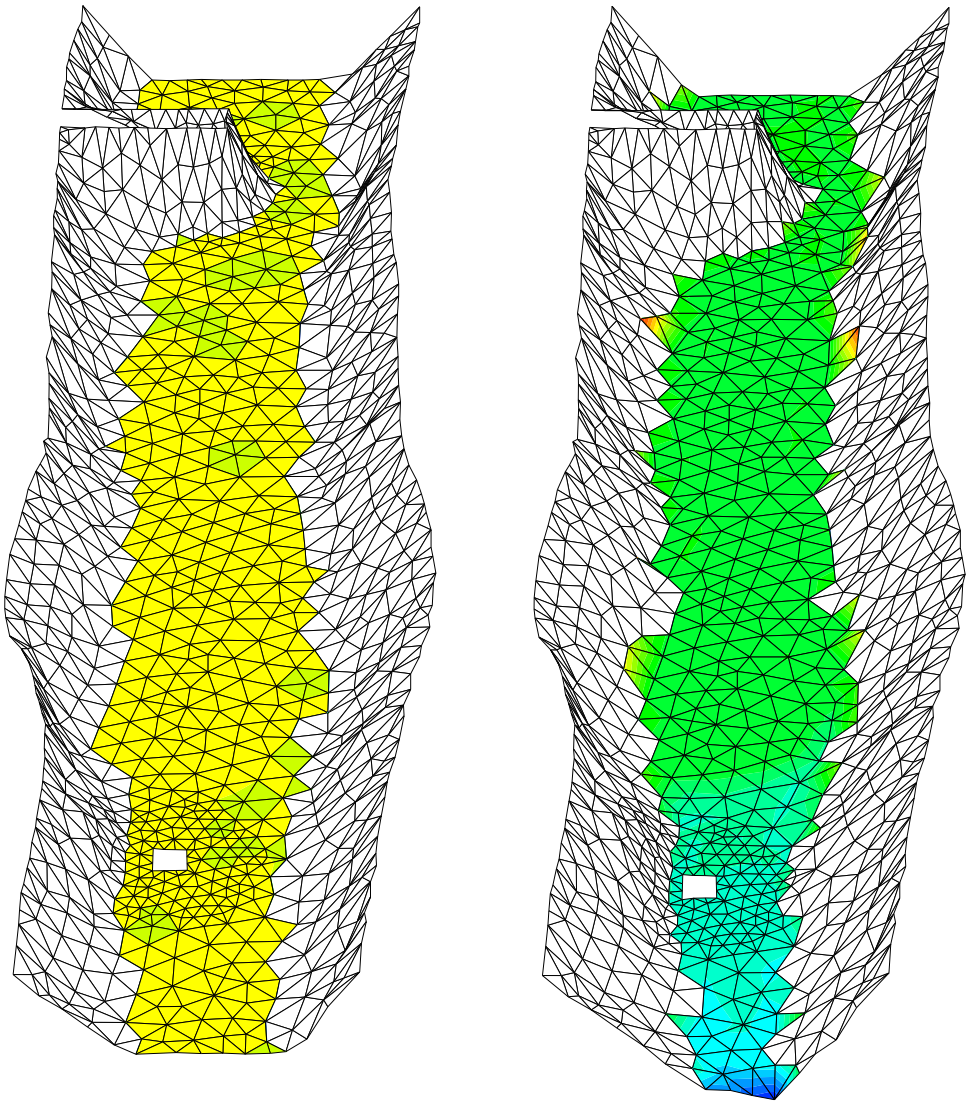

(a) Initial solution (b) $t = 2000$ s

Figure 8.5: Draining off the river (1).

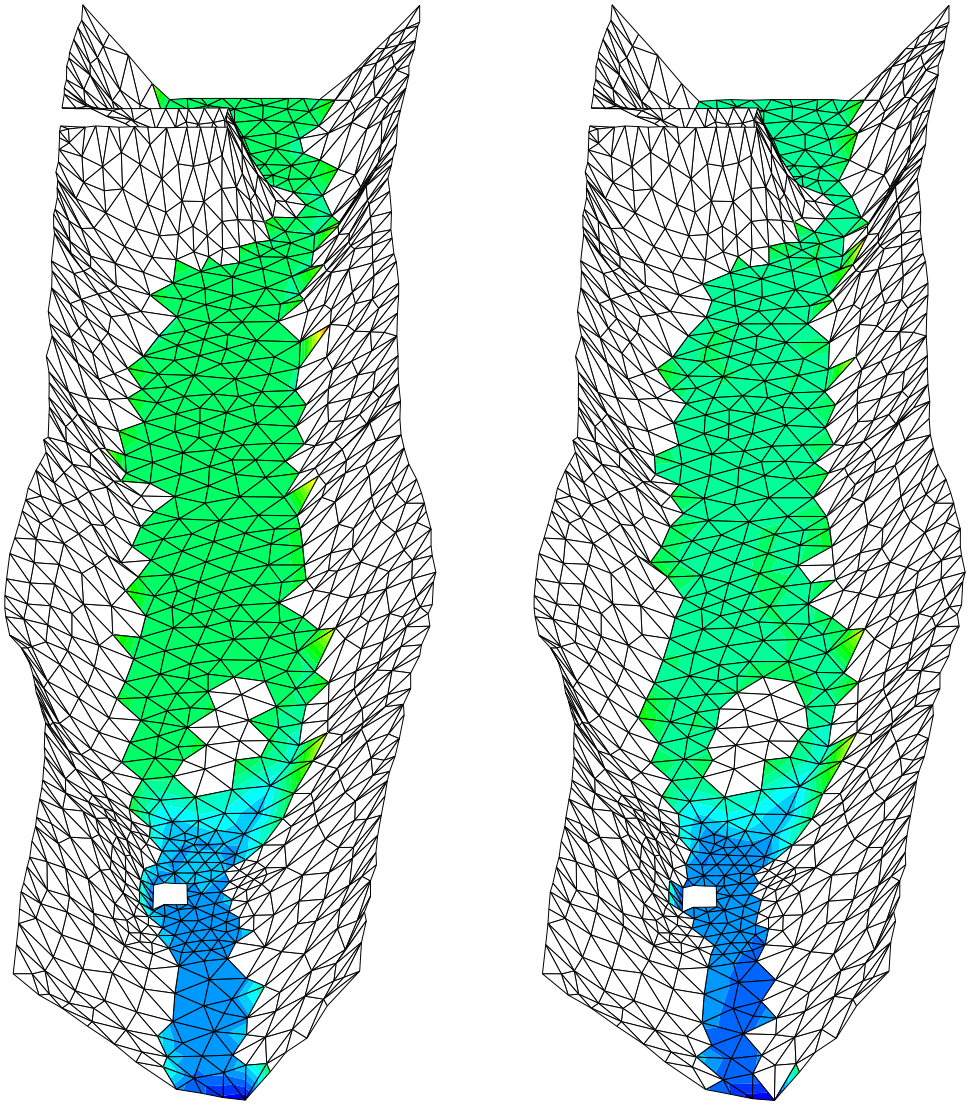

(a) $t = 5000$ s (b) $t = 8000$ s

Figure 8.6: Draining off the river (2).

A Study of functions $\phi(m)$ and $\psi(m)$

We recall that (see (6.21))

$$\phi(m) = \int_{(w_n \leq -\sqrt{2}m)\times \mathbb{R}} (\sqrt{2}m + w_n)\,\chi(w)\,dw \tag{A.1}$$

Using the definition (3.3) of $\chi(w)$ we have

$$\phi(m) = \begin{cases} \sqrt{2}m & \text{if m} \leq -\sqrt{\frac{3}{2}}, \\ -\frac{1}{2\sqrt{3}}(\sqrt{\frac{3}{2}} - m)^2 & \text{if } -\sqrt{\frac{3}{2}} \leq \text{m} \leq \sqrt{\frac{3}{2}}, \\ 0 & \text{if m} \geq \sqrt{\frac{3}{2}}. \end{cases} \tag{A.2}$$

We recall the definition (6.24)

$$\psi(m) = K\frac{(m+2)}{\phi(m)^{\frac{1}{3}}}, \tag{A.3}$$

so $\psi(m)$ is a C^1 function for $m < \sqrt{\frac{3}{2}}$.
Besides we have

$$\psi'(m) = \frac{K}{\phi(m)^{\frac{4}{3}}}\left(\phi(m) - \frac{1}{3}\phi'(m)(m+2)\right) \tag{A.4}$$

i.e for $m \leq -\sqrt{\frac{3}{2}}$,

$$\psi'(m) = \frac{K}{\phi(m)^{\frac{4}{3}}}\frac{2\sqrt{2}(m-1)}{3}, \tag{A.5}$$

and for $-\sqrt{\frac{3}{2}} \leq m < \sqrt{\frac{3}{2}}$,

$$\phi'(m) = -\frac{1}{\sqrt{3}}(m - \sqrt{\frac{3}{2}}), \tag{A.6}$$

$$\psi'(m) = \frac{K}{\phi(m)^{\frac{4}{3}}}\frac{1}{6\sqrt{3}}(m - \sqrt{\frac{3}{2}})(-m + 4 + 3\sqrt{\frac{3}{2}}). \tag{A.7}$$

So $\forall m \in]-\infty, \sqrt{\frac{3}{2}}[$, $\psi'(m)$ has the sign opposite of the one of K, the function $\psi(m)$ is monotonous.

Moreover we have

$$\begin{aligned} &\psi(m) \to +\infty \qquad \text{for m} \to \sqrt{\tfrac{3}{2}}, \\ &\psi(m) \to -\infty \qquad \text{for m} \to -\infty, \end{aligned} \tag{A.8}$$

so the equation (6.23) has a unique solution $m \in]-\infty, \sqrt{\frac{3}{2}}[$.

References

[1] Audusse E., Bristeau M. O. and Perthame B., Kinetic schemes for solving Saint-Venant equations with source terms, *Inria report*, RR-3989 (2000), http://www.inria.fr/RRRT/RR-3989.html

[2] Bristeau M. O. and Perthame B., Transport of Pollutant in Shallow Water using Kinetic schemes, ESAIM Proceedings, 10, CEMRACS 1999, pp 9–21, http://www.emath.fr/Maths/Proc/Vol.10.

[3] Coussin B., Etude des conditions aux limites pour la résolution numérique du système de Saint-Venant par un schéma cinétique, Rapport de stage, M3N, Inria, 2000.

[4] Dubois F. and Le Floch P., Boundary Conditions for Nonlinear Hyperbolic Systems of Conservation Laws, *J. Differential Equations*, 71, pp 93–122 (1988).

[5] Gallouët T., Hérard J.M. and Seguin N., Some approximate Godunov schemes to compute shallow-water equations with topography, AIAA-2001 (2001).

[6] Goutal N. and Maurel F. Proceedings of the 2nd workshop on dam-break simulation, Note technique EDF, HE-43/97/016/B (1997).

[7] Gerbeau J.-F. and Perthame B., Derivation of Viscous Saint-Venant System for Laminar Shallow Water; Numerical Validation, *Discrete Cont. Dyn. Syst. Ser. B*, 1, No 1, pp 89–102 (2001).

[8] Gisclon M. and Serre D., Conditions aux limites pour un système strictement hyperbolique fournies par le schéma de Godunov, *RAIRO Modél. Math. Anal. Numér.*, 31, pp 359-380, (1997).

[9] Godlewski E. and Raviart P.-A., *Numerical approximations of hyperbolic systems of conservation laws*, Applied Mathematical Sciences 118, Springer-Verlag, New York (1996).

[10] Hervouet J.M., TELEMAC modelling system: an overview, *Hydrol. Process.* 14, 2209–2210, (2000).

[11] LeRoux A.Y., Conditions aux limites et Problèmes Hyperboliques: un point de vue numérique, Workshop Conditions Limites Numériques pour les Systèmes Hyperboliques, I.H.P., Paris, Juin 2001.

[12] Perthame B., An introduction to kinetic schemes for gas dynamics, *An introduction to recent developments in theory and numerics for conservation laws.* L.N. in Computational Sc. and Eng., 5, D. Kroner, M. Ohlberger and C. Rohde eds, Springer (1998).

[13] Perthame B. and Qiu Y., A variant of Van Leer's method for multidimensional systems of conservation laws, *J. Comp. Phys.* 112(2), 370–381 (1994).

[14] Perthame B. and Simeoni C., A kinetic scheme for Saint-Venant equations with a source term, in preparation.

[15] Van Leer B., Towards the Ultimate Conservative Difference Schemes. V. A Second Order Sequel to the Godunov's Method, *J. Comp. Phys.*, 32 (1979).

Unit é de recherche INRIA Lorraine, Technop ôle de Nancy-Brabois, Campus scientifique,
615 rue du Jardin Botanique, BP 101, 54600 VILLERS L ÈS NANCY
Unit é de recherche INRIA Rennes, Irisa, Campus universitaire de Beaulieu, 35042 RENNES Cedex
Unit é de recherche INRIA Rh ône-Alpes, 655, avenue de l'Europe, 38330 MONTBONNOT ST MARTIN
Unit é de recherche INRIA Rocquencourt, Domaine de Voluceau, Rocquencourt, BP 105, 78153 LE CHESNAY Cedex
Unit é de recherche INRIA Sophia-Antipolis, 2004 route des Lucioles, BP 93, 06902 SOPHIA-ANTIPOLIS Cedex

Éditeur
INRIA, Domaine de Voluceau, Rocquencourt, BP 105, 78153 LE CHESNAY Cedex (France)
http://www.inria.fr
ISSN 0249-6399